# Structural mapping of Chikotra River basin in the Deccan Volcanic Province of Maharashtra, India from ground magnetic data

S P Anand[1,*], Vinit C Erram[1], J D Patil[2], N J Pawar[3], Gautam Gupta[1] and R A Suryavanshi[4]

[1]*Indian Institute of Geomagnetism, New Panvel (W), Navi Mumbai 410 218, India.*
[2]*DY Patil College of Engineering and Technology, Kolhapur 416 006, India.*
[3]*Shivaji University, Kolhapur 416 004, India.*
[4]*Y C College of Science, Karad 415 124, India.*
[*]*Corresponding author. e-mail: aerospl@yahoo.co.uk*

Ground magnetic data collected over Chikotra River in the peripheral region of Deccan Volcanic Province (DVP) of Maharashtra located in Kolhapur district was analysed to throw light on the structural pattern and distribution of magnetic sources within the basin. In order to isolate the magnetic anomalies showing varying trend and amplitude, several transformation operations including wavelength filtering, and upward continuation has been carried out on the reduced to pole anomaly map. Qualitative interpretation of these products help identify the distribution of magnetic sources, viz., the Deccan basalts, dolerite intrusives and older greenstone and schist belts in the subsurface. Present study suggests that the Chikotra basin is composed of three structural units; a NE–SW unit superposed on deeper NW–SE unit with randomly distributed trap flows on the surface. One of the major outcome of the present study is the delineation of almost 900-m thick Proterozoic Kaladgi sediments below the Deccan trap flows. The NE–SW magnetic sources may probably represent intrusives into the Kaladgi sediments, while the deeper NW–SE trends are interpreted as the northward extension of the Dharwars, underneath the Deccan lava flows, that forms the basement for the deposition of Kaladgi sediments.

## 1. Introduction

The Deccan traps of India, classified as large igneous province (LIP), which erupted during the KTB is one of the largest and best-exposed continental flood basalt provinces of the world. They consist of multiple layers of solidified flood basalt that together are more than 2000-m thick and cover an area of 500,000 km$^2$ and a volume of 512,000 km$^3$. A large portion of the west-central India is covered by the Deccan trap flows due to which little is known about the sub-trappean geology. On the south and south-east peripheral region of the Deccan trap lies the Proterozoic Kaladgi and Bhima basins, while the Gondwana Godavari basin lies on the east. These sedimentary basins may host minerals as well as hydrocarbons. Hence, it is of paramount importance to probe below the traps using geophysical methods. However, looking below basalt has always been a challenging problem for the Earth Science community. Recently, with the availability of sophisticated computers, data processing and imaging techniques, the interpretations have become further refined and have contributed to a quantum jump in the application of geophysical data, particularly aeromagnetic data, to sub-basalt exploration. Using advanced processing techniques on regional scale ground magnetic data from the eastern peripheral region of the Deccan traps, Rajaram *et al.* (2006)

**Keywords.** Magnetic anomalies; Dharwars; Kaladgi; Deccan lavas; filtering; Proterozoic.

*J. Earth Syst. Sci.* **125**, No. 2, March 2016, pp. 301–310

delineated the westward continuation of Archean structural elements below the traps, thus suggesting that magnetic data can provide sub-basalt information. In the present paper, we discuss a case study from the Chikotra basin located within the southern periphery of DVP, using ground magnetic data.

The Chikotra basin bounded by latitude 16°10′43″–16°27′202″ and longitude 74°8′9″–74°22′30″ lies in Kolhapur district of Maharashtra, occupying an area of approximately 351 km$^2$. Located approximately 50 km south of this basin is the Proterozoic intracratonic Kaladgi basin. The Kaladgi basin is important both in terms of uranium mineralization (www.amd.gov.in/regions/sr.htm) as well as hydrocarbons (Kalpana *et al.* 2010). However, the northward extension of the Kaladgi basin has not been mapped as it underlies the Deccan traps. The recent deep drilling in the Koyna region (KBH-1) has encountered ∼933 m trap overlying the granitic basement (Roy *et al.* 2013) with no infra-trappean sediments suggesting that the Kaladgi sediments are not extending up to Koyna. The Chikotra River lies between the deep borehole of Koyna towards the north and the exposed Kaladgi basin towards the south. In the present paper, an attempt has been made to look below the trap covered region of Chikotra basin using wavelength filtering and spectral techniques to throw light on the structural setup of the basin. Keeping the two objectives, i.e., structural mapping and delineating the presence of Proterozoic Kaladgi sediments, if any, below the trap cover, a ground magnetic survey was conducted over the Chikotra basin. Magnetic surveys can be used primarily to delineate buried igneous rocks and to locate faults within the basin fill (Grauch *et al.* 2001) as well as map the basement. It also helps construct the geometry of the subsurface as lithology controls magnetic properties through mineralogy and hence sharp variation in rock properties generally coincides with lithological contacts. Existence of faults/fractures in the subsurface geologic units creates magnetic variation and can produce anomaly in magnetic measurements. In the present study, the ground magnetic data collected over the Chikotra basin is qualitatively interpreted to delineate the structural pattern and trends and also to map the distribution of magnetic sources at shallow and deeper levels to throw light on the structure of the region.

## 2. Generalized geology and lithology

Physiographically, the study area comprises of hills on the southwestern side and plains on the northeastern side forming an irregular and diverse nature of topography of eastern flank of Western Ghats escarpment. Geologically, the basalts of the Deccan Volcanic Province (DVP) characterize the Chikotra basin (figure 1a). In general, the basaltic flows are of simple type with few tens of meters as the thickness of simple flows is much less and does not exceed 30–40 m (Mungale 2001). The basalts from the area are dark to grey in colour and fine to medium-grained in texture. They show typical spheroidal weathering that gives rise to large rounded boulders on the outcrops. The flows have been separated by thin clayey horizons of tuffaceous aspect called as the redbole beds. The thickness of the redbole beds varies from $< 2.5$ to 1 m. In some parts, the topographic highs have been covered with laterite and in the downstream part by a thin veneer of alluvium, which is developed along the banks of the Chikotra River and streams (Mungale 2001). The alluvium mainly occurs along the slopes of the hills, along the banks of the Chikotra River. The thickness of alluvium varies from 2 to 6 m, which gradually increases in the downstream areas where the Chikotra River meets the Vedganga River. The laterite occurs as capping over the flat topped basaltic hills, at the upstream part in the source of Chikotra River at an elevation of about 905 m amsl. The drainage pattern is not uniform in the basin. In the upstream areas, the pattern is dendritic and fine-textured. This type of drainage pattern is usually observed on horizontally disposed basaltic rock that is uniformly resistant with gentle regional slope (Horton 1945). Near surface (∼10 m) hydrogeological section (Gupta *et al.* 2015) generated from available dug well and borehole distributed randomly in the basin suggest that the top layer comprises red bole, laterite or black soil, followed by weathered or fractured rock grading into compact basalts. In a regional geologic scenario (figure 1b), to the southeast of Chikotra basin, lies the Proterozoic Kaladgi basin with maximum aggregate sediment thickness of approximately 4500 m (Jayaprakash *et al.* 1987; Radhakrishna and Vaidyanadhan 1997). Several exposures of Kaladgi formations are seen around the Chikotra basin. The basin exposes sediments of older, highly deformed, Bagalkot group (major lithology includes ortho-quartize, shale, dolomite and limestone) and younger, underformed Badami group comprising conglomerate, arenite, shale and limestone (Kalpana *et al.* 2010, www.amd.gov.in/regions/sr.htm). The Simikeri subgroup of Kaladgi formations hosts acidic and basic intrusives (Jayaprakash *et al.* 1987). The basic intrusives are represented by dolerite dykes and are considered pre-Badami and post-Bagalkot in age. Some of the outcropping dykes are reported to have strike length of 3–5 km and are either parallel or at acute angle to the enclosing formations (Jayaprakash *et al.* 1987). Kerkalmatti member of Simikeri subgroup

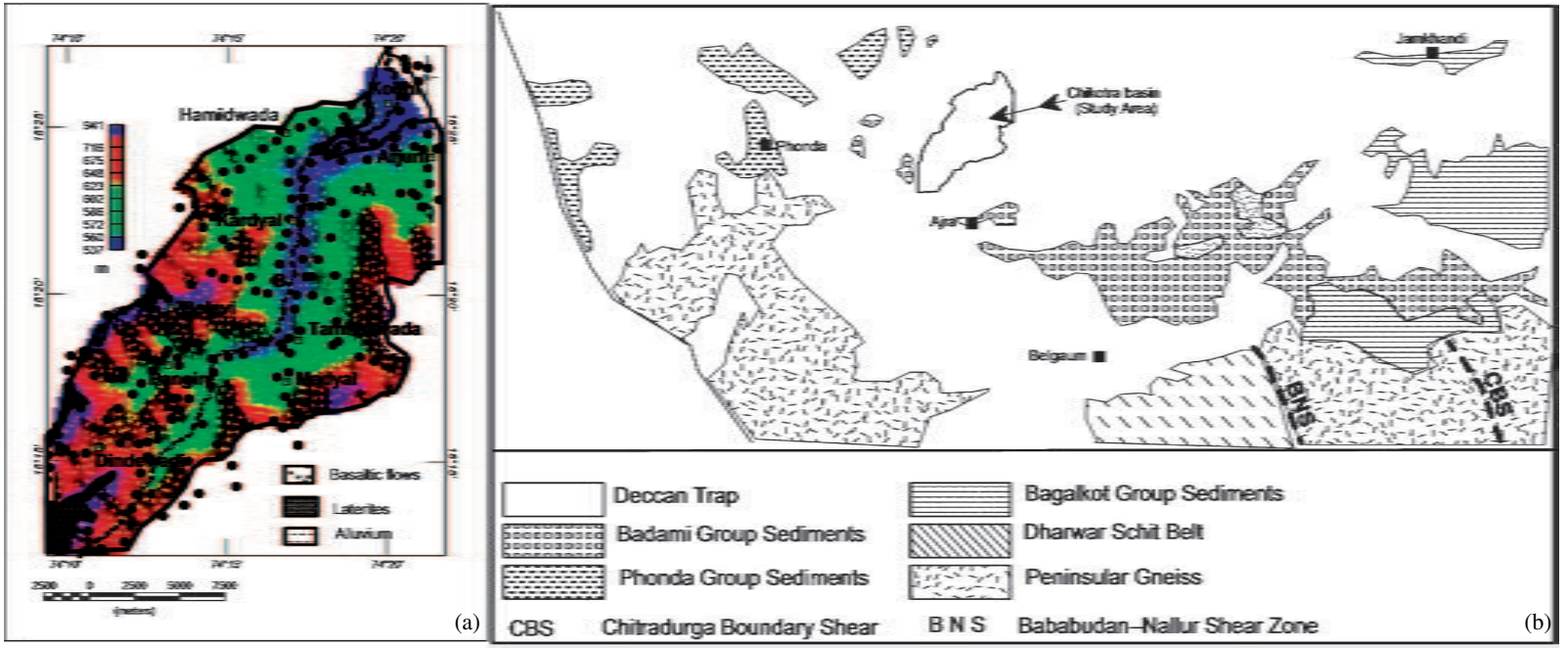


Figure 1. (**a**) Generalized geological map of the Chikotra basin superposed on the topographic map. Solid circle represents data distribution. (**b**) Regional geological map in and around the Chikotra basin showing the exposed Proterozoic Kaladgi formations and the supra crustals associated with the Dharwar super group (redrawn from www.amd.gov.in/regions/sr.htm and GSI 2001).

is characterized by approximately 50-m thick Hematite schist at a depth of 2 km distributed throughout the basin. The shales of the Lokapur subgroup of the Bagalkot group are enriched with MgO, $Fe_2O_3$, Cr, Ni, Co and Sc suggesting that the early sediments were derived from a more mafic provenance (Rao *et al.* 1999). Achaean peninsular gneisses, Chitradurga schists of Dharwar super group and intrusive Closepet granite and its equivalents form the basement rocks for the Proterozoic Kaladgi sediments. E–W, NE–SW and NW–SE trending faults and fractures have affected both basement rocks and the sediments (www.amd.gov.in/regions/sr.htm). The Bababudan–Nallur Shear (BNS) separates the greywackes and conglomerates of the Dharwar Schist belt in the west from the older (3 Ga) Peninsular Gneissic complex towards the east (Ramadass *et al.* 2004), while Chitradurga Boundary Shear (CBS) (GSI 1994; Gokarn *et al.* 2004)/Closepet granite (Swami Nath *et al.* 1976; Subrahmanyam and Verma 1982) is considered as the divide between eastern and western Dharwar Craton. The Peninsular Gneissic complex is composed of Tonalite–Trondhjemite–Granodiorite suites (Radhakrishna and Vaidyanadhan 1997).

## 3. Magnetic data and methodology

Total field magnetic data were collected over 200 locations using proton precession magnetometer having a resolution of 0.1 nT over Chikotra basin with an average station spacing of 600 m and dictated by road access. The magnetic measurements made at any point contains contribution from three major sources: the main (core) field (corrected using International Geomagnetic Reference Field models), the external field (diurnal corrections using data from base station magnetometer or data from nearby magnetic observatory) and the crustal field. The total field crustal anomaly map generated using a 440 m grid (grid size calculated taking into account the number of data points and the total area), after applying necessary corrections to the observed data, is represented as a histogram equalized image map (figure 2). Regions where the distance between two data points is more than 3500 m (inaccessible terrain) is blanked (white patches in figures). The magnetic anomaly map shows a mixture of several high amplitude medium wavelength anomalies along with medium to high amplitude short wavelength anomalies. Anomalies, in general strike in a NE–SW direction, with minor NW–SE trends. Mixture of different frequencies and trends suggests that the causative sources are different and occurring at different depth levels. The interpretation of total field magnetic anomalies is not straightforward as the ambient field direction changes with location (Blakely 1995).

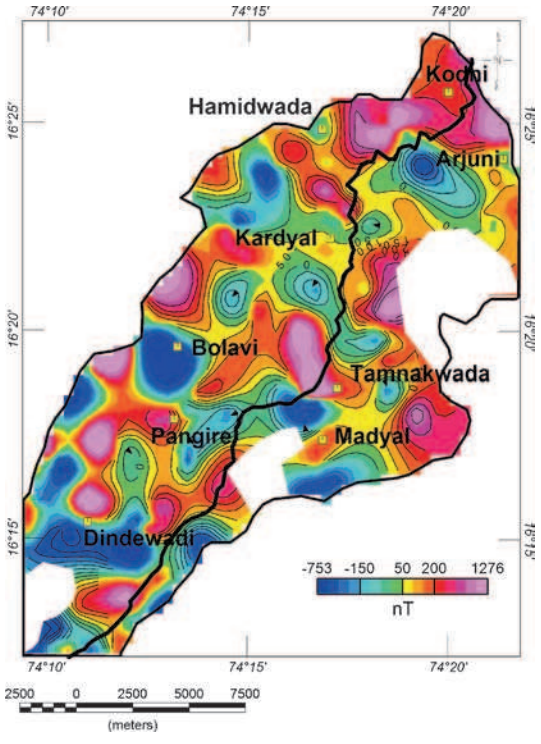


Figure 2. Histogram equalized crustal magnetic anomaly map of Chikotra basin.

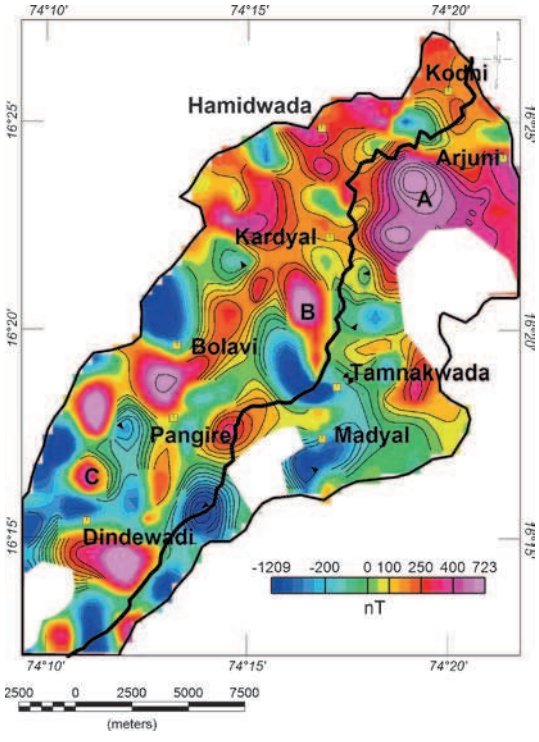


Figure 3. Reduced to pole (RTP) anomaly map of Chikotra basin. Solid line represents Chikotra river. Half-filled circle shows the location of borewell referred in the text. A, B, C refer to anomalies discussed in the text.

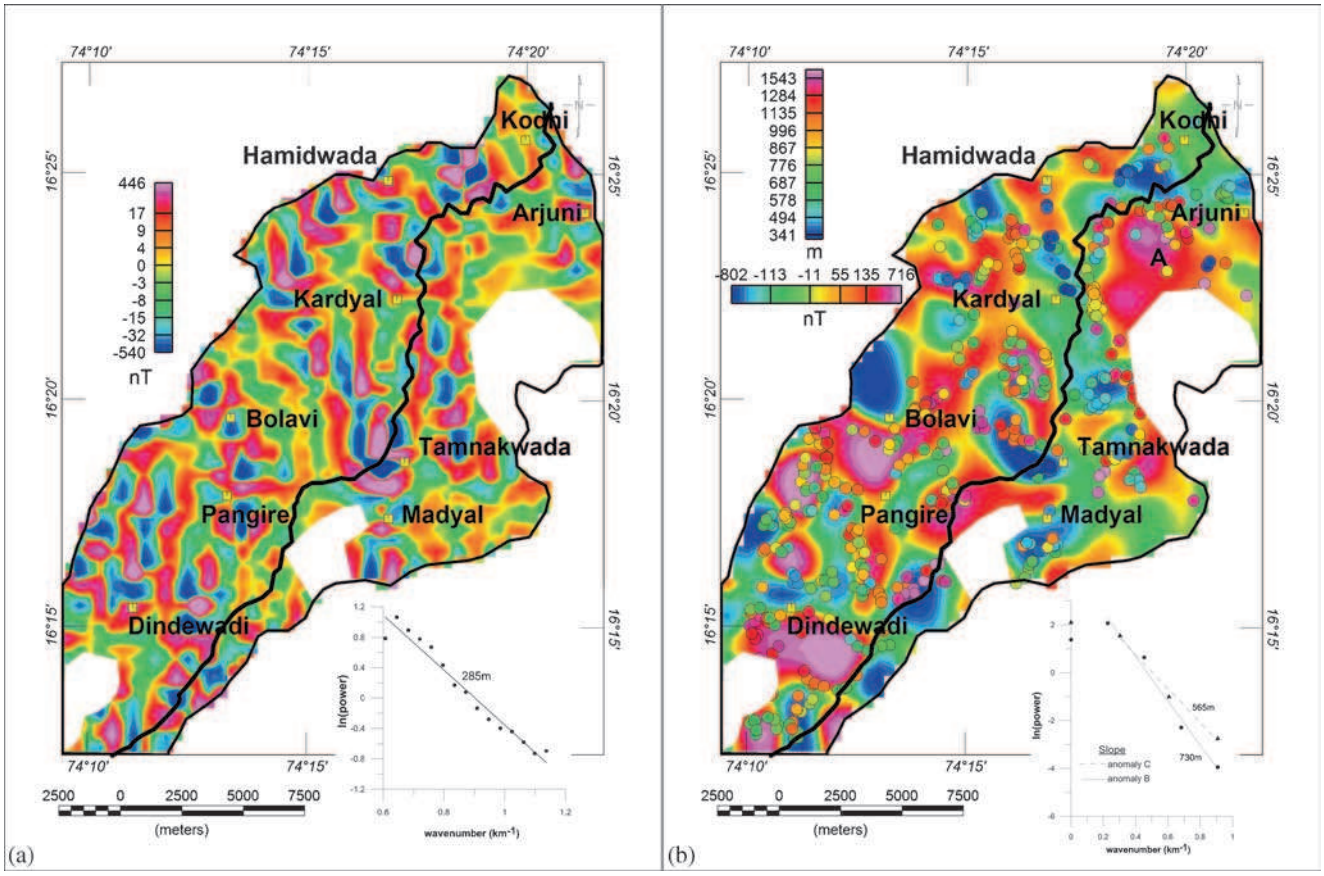


Figure 4. (**a**) Butterworth high-pass filtered anomaly map. Inset shows the radially-averaged power spectrum of the high-pass filtered data. (**b**) Butterworth band-pass filtered map with cut-off wavelength 1.8–13 km. Inset shows the radially-averaged power spectrum computed for anomalies B and C assuming prism model. Vertical scale bar shows depth calculated using Euler deconvolution for SI = 1 and horizontal scale bar band pass filtered magnetic anomaly.

In the present study area, the inclination of the total field changes from 21.04° to 21.59° with a mean of 21.32°. Because of this changing inclination, the anomalies may not be falling directly over the causatives. Hence, a reduction to pole operation (Silva 1986) was carried out to get rid of the bipolar nature of the anomalies, thereby placing the anomalies directly over the causatives. As the region under study is falling in the low magnetic latitudes, we have utilized the pseudo-inclination method (MacLeod 1993; Xiong Li 2008), where a pseudo-inclination higher than the actual inclination is specified to suppress the amplitude of the noise along the direction of declination. Reduced to Equator (RTE) is another option but the RTE maps are more complex to interpret (Xiong Li 2008), hence we have not utilized RTE. Reduced to Pole (RTP) anomaly map thus generated using mean inclination of 21.32° and a declination of –1.031° (for the present geomagnetic field) is shown in figure 3. The anomalies in the RTP map shows a combination of NW–SE and NE–SW trends with varying wavelength and amplitude suggesting different levels of occurrence of the causatives. Hence, to separate out the magnetic anomalies arising from different depth levels, transformation operations (Blakely 1995), which accentuates certain characteristics of the anomalies, were carried out on the reduced to pole anomaly data to get better insight of the causative source. Anomaly maps generated using these transformation operations can be utilized for qualitative interpretation and build a tectonic model of the region under study. In the present study, we have used wavelength filters and upward continuation for isolating the magnetic sources at different depth levels. To get an idea of the average depth to the sources at different depth levels, radially averaged power spectrum was computed from the 2D spectrum of the wavelength filtered (high-pass and low-pass), reduced to pole anomaly data. Slope of the power spectrum will give average depth to the top of different layers (Blakely 1995) with different susceptibility contrast. The computed radially-averaged power spectrum from the magnetic data can be divided into several straight line segments, the

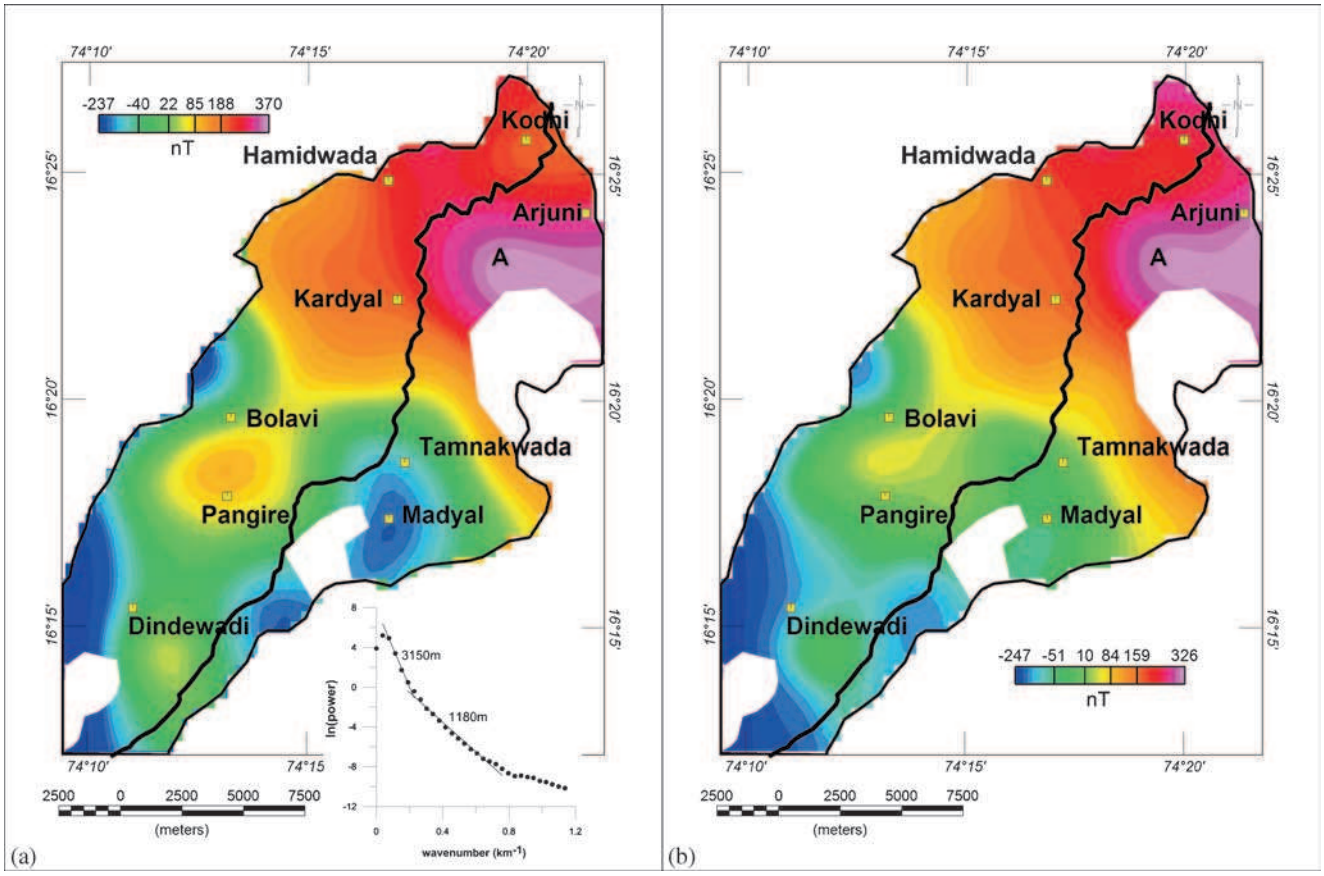


Figure 5. (**a**) Low-pass filtered RTP anomaly map with cut-off wavelength of 13 km. Inset shows radially-averaged power spectrum computed for the low-pass filtered map. The depth related to the second segment is referred in the text. (**b**) RTP anomaly map upward continued to 2 km representing deeper sources.

slope of each segment giving the average depth of the corresponding layers (Spector and Grant 1970) with different magnetizations. In the present study, the slope of the line segments were accepted only if the coefficient of determination of the fit is greater than 0.96, otherwise discarded. In addition to power spectral method, 3D Euler deconvolution technique was also applied to the RTP anomaly data to determine the position and depth of the magnetic source present. The method solves Euler's homogeneity equation (Reid *et al.* 1990) for source position, working on a moving window on the grid. The data was re-gridded at 200 m interval as the original grid of 440 m gave very less solution for different structural index. Depth estimates have been carried out for the whole basin using Euler deconvolution technique assuming structural index of 0, 0.5, 1 and 2. Better solution clustering was obtained for SI = 1, which is superposed on figure 4(b).

The RTP anomaly map (figure 3) shows several interesting features having NE–SW, NW–SE and NS trends. The anomaly map is dominated by medium to long wavelength anomalies; it is interesting to mention that high-frequency high–low paired anomalies which represent the Deccan trap flows (Anand and Rajaram 2007) as seen in thick trap covered regions is not easily identifiable in the anomaly map. By and large, the high amplitude anomalies are found to lie on the northern part of the Chikotra River, while the region below the river is essentially smooth except for the long wavelength anomaly A, whose amplitude is the highest (∼500 nT). This can possibly represent a region of uplift or a change in lithology. Low amplitude anomaly closures seen near Madyal and Tamnakawada may possibly represent subsurface localized basins or intrusive, having high remnant magnetism. As the RTP anomaly map contains magnetic signatures from sources distributed at different depth levels, a Butterworth high, low and band pass filter was designed, to separate the magnetic sources at different depth levels. The filter parameters (cut-off wavelength and order of filter) was designed through trial and error method. A Butterworth high-pass filter with cut-off wavelength of 1800 m, Butterworth band-pass filter with cut-off wavelengths between 1800 and 13,000 m and low-pass filter that passes

all wavelengths above 13,000 m was used for separating the magnetic sources at different depth levels and are shown in figures 4(a, b) and 5(a). For the cut-off wavelengths <1800 m and >13000 m, we have calculated the depths using radially averaged power spectrum and these are shown as inset in figures 4(a) and 5(a). The high-pass filtered map shows several high amplitude anomalies with peak to peak amplitudes of over 990 nT suggesting highly magnetized sources at very shallow levels. The average depth of this layer calculated from the radially averaged power spectrum is 285 m. Majority of the anomalies seen on the RTP map is reproduced in the band-pass filtered map (figure 4b) suggesting that most of the causatives are at intermediate depth levels. Most of the anomalies in the band-pass filtered map are either circular or slightly elliptical, which suggest geometries related to intrusive in the subsurface. Radially averaged power spectrum of two individual anomalies (B, C), assuming deterministic model (Mishra 2011) instead of statistical models, suggests that the depth of the causatives associated with B is 730 m, while that of C is 565 m. The depth to the top of sources generated using Euler deconvolution with SI of 1 are superposed on figure 4(b). The average depth to the top of the causatives calculated using Euler deconvolution is 680 m.

The regional map generated using low pass filtering (figure 5a) and upward continuing the RTP map to 2000 m (figure 5b) trends essentially in the NW–SE direction and the anomalies represent causatives at deeper levels. There are no NE–SW anomalies observed on these maps, suggesting that the causatives responsible for the NE–SW trends are shallower in origin. The average depth to this layer is 1180 m as deduced from the radially-averaged power spectrum.

## 4. Discussion

Ground magnetic data collected over the Chikotra River has been processed to throw light on the structural setting of the region. From the RTP anomaly map and its transformations, we found that the major sources of the magnetic anomaly in the region are distributed at three different depth levels, viz., 285, ∼700 and 1180 m deduced from the radially-averaged power spectrum of the wavelength filtered RTP maps. Few borewells have been drilled in the area for irrigation purpose whose information inferred from interaction with local farmers, were utilized to prepare subsurface litho sections. The litho section from a borehole drilled near Madyal which penetrated up to a depth of 72 m has shown the presence of volcanic breccia sandwiched between jointed basalts, while the litho sections from two boreholes south of Arjuni include thin layer of soil, followed by weathered jointed basalt, redbole and compact basalt. These wells have penetrated to a depth of 108 and 150 m respectively. Another borehole drilled near Tamnakawada (represented by half-filled circle in figure 3), encountered sandstone of Kaladgi formation after penetrating almost 160 m of trap flows. Compared to weathered and jointed basalts, compact basalts give higher susceptibilities. Hence, we interpret that the regions reflecting high frequency anomalies may possibly represent areas of thick compact basalts in the subsurface. It can be seen that majority of compact basalts at shallower level are located towards the north (region above) of Chikotra River compared to south. For such a distribution of compact basalts, two scenarios are possible: (a) a major fault along the Chikotra River, Chikotra River Fault (CRF), along which the compact basalts are down thrown towards the south and (b) the jointed/weathered basalts are thicker towards

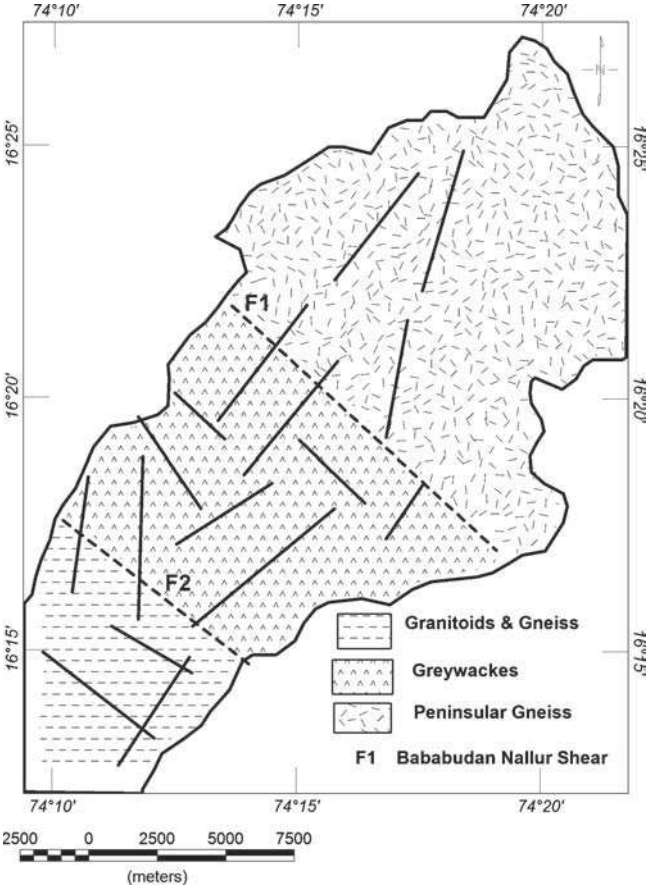


Figure 6. Interpreted structural and lithological map of Chikotra basin from magnetic data and its transformations. Dashed lines represent deep seated faults/lineaments, while shallower faults/lineaments/contacts are represented by continuous lines.

the south. By and large, the resistivity modelling (Gupta *et al.* 2015) also shows high resistivity representing compact basalts at shallow levels in the region north (region above) of the Chikotra River, while it is at deeper levels to the south of the river. Magnetic sources associated with second layer which is at an average depth of 700 m trends in NE–SW and NW–SE direction. The sources of these anomalies can be the following: (1) pre-Badami and post-Bagalkot basic dolerite dykes that are intruded into the Kaladgi sediments (Jayaprakash *et al.* 1987) or (2) iron-magnesium enriched shales in the lower group of the Kaladgi formations. Major, trace and rare earth element geochemical studies (Rao *et al.* 1999) have shown that the lower group (Lokapur) shales of Kaladgi formations are characterized by higher $Fe_2O_3(t) + MgO$ and associated elements. Further detailed geophysical investigations are required to confirm the present inferences. Deeper sources (∼1180 m) are showing NW–SE trends as evidenced in the upward continued and low pass filtered anomaly maps. The effect of the CRF in controlling the structural disposition of the anomalies is evident even in the deeper structural elements. Hence, we infer that the CRF is a deep seated fault, probably involving the basement. In the regional geologic picture, NW–SE features represent the trends of the Dharwar formation and hence, we infer that these NW–SE trends at deeper levels as the northward continuation of the Dharwar formation underneath the Deccan trap flows. Two major lineaments/faults, F1 and F2 are inferred from the low pass filtered RTP anomaly map and upward continued map that delineates deeper sources and is shown in figure 6. On comparison with the regional tectonic elements (figure 1), it appears that the F1 coincides with the northwest continuation of Bababudan–Nallur Shear (BNS) that divides the Dharwar Schists belt from the Peninsular Gneissic complex composed of tonalite–trondhjemite–granodiorite. This interpretation is supported by the ground magnetic studies conducted by Ramadass *et al.* (2004), along a profile running from Goa to Jedcherla, towards south of the present study region. The BNS shows signatures even in the radiometric anomalies (Himabindu and Ramadass 2003). F2 can either be a fault within the Dharwar Schist Belt or the lithological contact between the greywackes on the east and granitoid and gneiss towards the west. A structural trend and fault distribution map generated from the combination of RTP map and its transformations is represented in figure 6. A sketch representing a possible geological model, synthesized from the present study, is shown in figure 7. From the present study, we have

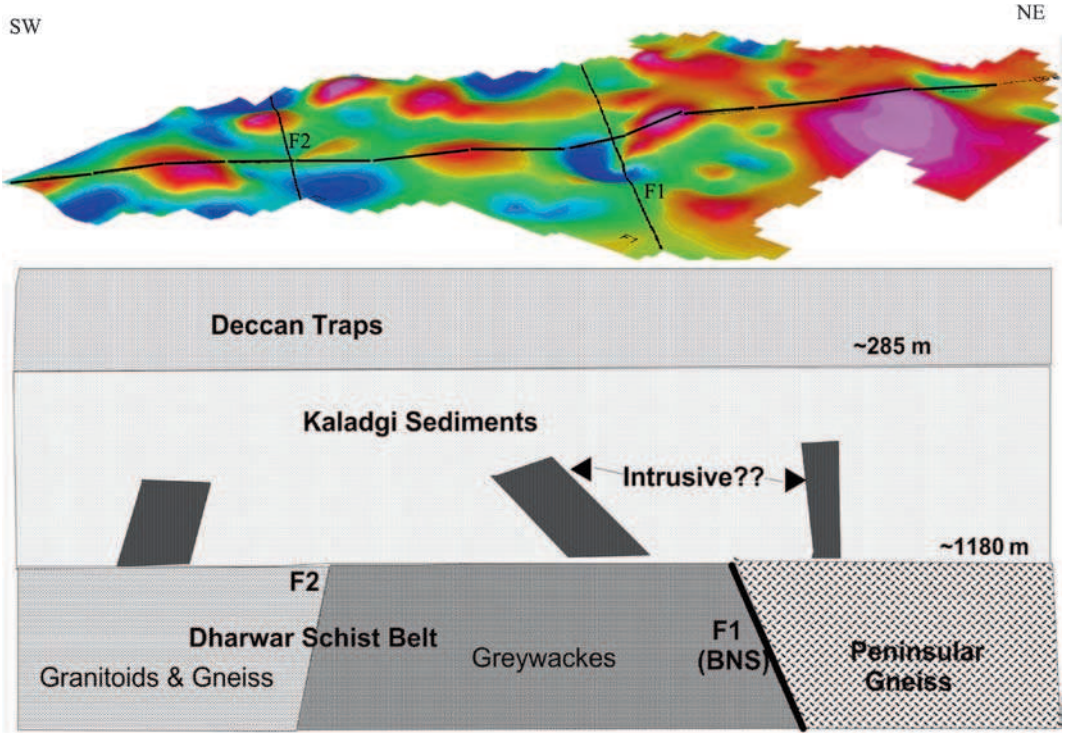


Figure 7. Sketch showing a possible geological cross section along an NW–SE profile overlain by the 3D perspective of reduced to pole map. Cool colour in the perspective map represents lows and warm colour highs. For scale please refer figure 3. F1 and F2 represent deep-seated faults inferred from the present study. F1 corresponds to Bababudan–Nallur Shear (BNS). The dimensions and dip of the intrusives are arbitrary.

delineated the presence of almost 900 m Proterozoic sediments of Kaladgi basin below the trap flows in the Chikotra basin. The borewell drilled for irrigation purpose has confirmed the presence of Kaladgi sandstones at a depth of 160 m below the basaltic flows. It is worth mentioning that geochemical studies conducted in the Kaladgi basin (Kalpana *et al.* 2010) has revealed occurrence of anomalous concentrations of light gaseous hydrocarbons in the near surface soil suggesting that the Kaladgi basin may be a potential basin. Also, aeromagnetic and radiometric surveys over the eastern and western part of the exposed Kaladgi basin has shown that the basin has the ideal geological setting to host typical unconformity type uranium deposits (www.amd.gov.in/regions/sr.htm).

Synthesizing the results from the present analysis, it can be inferred that the Chokotra River, in the Deccan trap covered region, is composed of three structural units. The upper unit representing the Late Cretaceous Deccan lava flows, followed by an intermediate layer having NE–SW structures and faults associated with the Proterozoic Kaladgi basin and the deeper unit representing the northwest continuation of the Dharwarian lithology. The basin area is characterized by approximately 285-m thick basaltic flows followed by almost 900-m thick Kaladgi sediments resting on the Archeans of the Dharwar craton.

## 5. Conclusion

The present study helps to throw light on the magnetic stratigraphy of the Chikotra basin in the proximity of the outcropping Kaladgis. The salient findings from the present study are: (a) Chikotra basin area is composed of three structural units: an intermediate NE–SW unit superposed on regional NW–SE unit and a shallow high amplitude magnetic sources representing Deccan trap flows, (b) the northward extension of the Dharwar craton underneath the Deccan trap, and (c) delineation of approximately 900 m Proterozoic Kaladgi sediments below the trap flows.

## Acknowledgements

The authors are thankful to the Director, Indian Institute of Geomagnetism for the support and the permission to publish this work. SPA is thankful to Dr L K Das for valuable discussions. They thank the three anonymous referees for their meticulous reviews and suggestions which have greatly improved the paper.

## References

Anand S P and Rajaram M 2007 Aeromagnetic signatures of the cratons and mobile belts over India; *Int. Assoc. Gond. Res. Mem.* **10** 233–242.

Behera L and Sen M K 2014 Tomographic imaging of subbasalt Mesozoic sediments and shallow basement geometry for hydrocarbon potential below the Deccan Volcanic Province (DVP) of India; *Geophys. J. Int.* **199** 296–314.

Blakely R J 1995 Potential theory in gravity and magnetic applications; Cambridge University Press, Australia.

Bois C, Bouche P and Pelet R 1982 Global geologic history and distribution of hydrocarbon reserves; *AAPG Bull.* **66** 1248–1270.

Grauch V J S, Hudson M R and Minor S A 2001 Aeromagnetic expression of faults that offset basin fill, Albuquerque basin, New Mexico; *Geophysics* **66** 707–720.

GSI 1994 Project Vasundhara, Spec. Publ. AMSE Wing, Geol. Surv. India, Bangalore.

GSI 2000 Aeromagnetic image of a part of peninsular India; *Geol. Surv. India* (scale l:2.000,000).

Geological Survey of India (GSI) 2001 Seismotectonic Atlas of India and its Environs, Bangalore, scale 1:1 million.

Gokarn S G, Gupta G and Rao C K 2004 Geoelectric structure of the Dharwar craton from magnetotelluric studies: Archean suture identified along the Chitradurga–Gadag schist belt; *Geophys. J. Int.* **158** 712–728.

Gupta G, Patil J D, Maiti S, Erram V C, Pawar N J, Mahajan S H and Suryawanshi R A 2015 Electrical resistivity imaging for aquifer mapping over Chikotra River basin, Kolhapur District, Maharashtra; *Environ. Earth Sci.* **72(12)** 8125–8143.

Himabindu D and Ramadass G 2003 A note on the qualitative appraisal of radiometric investigations along the Goa-Kushtagi profile; *J. India Geophys. Union* **7** 37–41.

Horton R E 1945 Erosional development of streams and their drainage basins: Hydrophysical approach to quantitative morphology; *Geol. Soc. Am. Bull.* **56** 275–370.

Jayaprakash A V, Sundaram V, Hans K and Mishra R N 1987 Geology of Kaladgi–Badami Basin, Karnataka; In: Purana Basins of Peninsular India, *Geol. Soc. India Memoir* **6** 201–225.

Kalpana M S, Patil D J, Dayal A M and Raju S V 2010 Near surface manifestation of hydrocarbons in Proterozoic Bhima and Kaladgi basins: Implications to hydrocarbon resource potential; *J. Geol. Soc. India* **76** 548–556.

MacLeod I N, Jones K and Dai T T 1993 3D analytic signal in the interpretation of total magnetic field data at low magnetic latitudes; *Explor. Geophys.* **24** 679–687.

Mishra D C 2011 Gravity and magnetic methods in geological studies: Principles, integrated exploration and plate tectonics; B.S. Publications, Hyderabad, ISBN: 978-93-81075-27-2.

Mungale S 2001 Geology of the Chikotra basin with special reference to watershed development; Unpublished dissertation, Department of Geology, University of Pune, 63p.

Radhakrishna B P and Vaidyanadhan R 1997 *Geology of Karnataka*, Text book series, Geol. Soc. India, Bangalore.

Rajaram M, Anand S P and Balakrishna T S 2006 Composite magnetic anomaly map of India and its contiguous regions; *J. Geol. Soc. India* **68** 569–576.

Ramadass G, Himabindu D and Ramaprasada Rao I B 2004 Magnetic basement along the Jadcharla–Vasco transect, Dharwar Craton, India; *Curr. Sci.* **86(11)** 1548–1553.

Rao S V V, Sreenivas B, Balaram V, Govil P K and Srinivasan R 1999 The nature of the Archean upper crust as revealed by the geochemistry of the Proterozoic shales of the Kaladgi basin, Karnataka, southern India; *Precamb. Res.* **98** 53–65.

Reid A B, Allsop J M, Granser H, Miliett A J and Somerton W I 1990 Magnetic interpretations in three dimensions using Euler deconvolution; *Geophys.* **55** 80–91.

Roy S, Rao N P, Akkiraju V V, Goswami D, Sen M, Gupta H, Bansal B K and Shailesh Nayak 2013 Granitic basement below Deccan Traps unearthed by drilling in the Koyna seismic zone, western India; *J. Geol. Soc. India* **81** 89–90.

Roy T K 1991 Structural styles in southern Cambay basin, India and role of Narmada geofracture in formation of giant hydrocarbon accumulation; *ONGC Bull.* **27** 15–56.

Sain K, Zelt C A and Reddy P R 2002 Imaging of subvolcanic Mesozoics in the Saurashtra peninsula of India using travel time inversion of wide-angle seismic data; *Geophys. J. Int.* **150** 820–826.

Silva J C B 1986 Reduction to the pole as an inverse problem and its application to low latitude anomalies; *Geophys.* **51(2)** 369–382.

Spector A and Grant F S 1970 Statistical models for interpreting aeromagnetic data; *Geophysics* **35** 293–302.

Subrahmanyam C and Verma R K 1982 Gravity interpretation of the Dharwar greenstone-gneiss-granite terrain in the southern Indian shield and its geological implications; *Tectonophys.* **84** 225–245.

Swami Nath J, Ramakrishnan M and Viswanatha M N 1976 Dharwar stratigraphic model and Karnataka craton evolution; *Rec. Geol. Surv. India* **107** 149–175.

Xiong Li 2008 Magnetic reduction to the pole at low latitudes: Observations and considerations; *Lead. Edge.* **27(8)** 990–1002.

*MS received 15 February 2015; revised 21 August 2015; accepted 26 October 2015*